Journal of Applied Mathematics and Computation, 2024, 8(3), 191-201
https://www.hillpublisher.com/journals/JAMC/
ISSN Online: 2576-0653
ISSN Print: 2576-0645

Effect of Physical Parameters and Tilt Angle on Nusselt Number

Madialène Sene[1,*], Momath Ndiaye[1], Goumbo Ndiaye[2]

[1]Hydraulics, Rural Engineering, Machinery and Renewable Energies Training and Research Unit, University of Sine Saloum El Hadj Ibrahima NIASS, 5V7F+JH3, Kaolack, Senegal.
[2]Sen'eau, BP 4945, Dakar, Senegal.

How to cite this paper: Madialène Sene, Momath Ndiaye, Goumbo Ndiaye. (2024) Effect of Physical Parameters and Tilt Angle on Nusselt Number. *Journal of Applied Mathematics and Computation*, 8(3), 191-201.
DOI: 10.26855/jamc.2024.09.001

Received: July 31, 2024
Accepted: August 30, 2024
Published: September 29, 2024

***Corresponding author:** Madialène Sene, Hydraulics, Rural Engineering, Machinery and Renewable Energies Training and Research Unit, University of Sine Saloum El Hadj Ibrahima NIASS, 5V7F+JH3, Kaolack, Senegal.

Abstract

Using a conformal transformation, our curvilinear boundary domain is reduced to a parallelepiped domain to formulate boundary conditions more simply without increasing the complexity of the formulation of equations. The authors numerically study natural steady-state thermal convection within an enclosure bounded by two portions of cylindrical horizontal generator dishes and a flat surface. To generalize the problem and reduce the number of parameters involved, the equations will be dimensionalized thanks to carefully chosen reference quantities. Nonlinear algebraic systems resulting from discretization by the PDQ Method are solved by an iterative line-by-line relaxation method. Estimates of the space steps that give our schemes high stability are given. The authors analyzed the effects of control parameters such as the Rayleigh number and the variation in the mean Nusselt number as well as the variation in the local Nusselt number.

Keywords

Convection; PDQ method; Rayleigh number; Nusselt number

1. Introduction

Over the past six decades, considerable effort has been devoted numerically and experimentally to the study of natural convection in finite geometries. Interest in these problems stems from their importance in areas such as applications in solar energy sensors, thermal storage systems, cooling of electronic components, design of nuclear reactors, and many other situations.

Even after 60 years of research, most research found in the literature is related to regular shapes like a square, or cylindrical ring. Due to the complexity of natural convection in non-rectangular and non-cylindrical types of enclosures, especially curved boundary enclosures, very few studies have been found. The first work on digital natural convection was undertaken in the 60s by G. de Vahl Davis et al. [1]. They used the finite difference method to solve the problem of natural convection in a differentially heated square cavity. These authors showed for Rayleigh number values less than 10^4, the temperature distribution at mid-height of the cavity is almost linear, and the vertical thermal gradient tends towards zero. At the end of the eighties, and thanks to the development of computers, G De Vahl [2] proposed a standard solution called Benchmark.

Kaviany [3] showed that the presence of a semi-cylindrical protuberance at the bottom of a square cavity decreases the rate of heat transfer on this surface. Lewandowsky [4] who uses a cylindrical cavity whose bottom is hemispherical, observes that compared to a conventional cylinder, we can amplify or attenuate the heat transfer inside the enclosure. By studying unsteady laminar natural convection inside an air-filled vertical axisymmetric ellipsoid, Najoua et al. [5] showed that the mean instantaneous Nusselt number decreases monotonically over time when the flow is unicellular and increases or decreases sharply with each appearance or disappearance of cells. Das and Morsi [6, 7] digitally studied constant two-dimensional natural convection inside a domed enclosure. In this study, domes of circular, elliptical, parabolic, and hyperbolic shapes were taken into account.

Kumar and Reddy [8] numerically analyzed combined natural convection and radiant heat loss in a parabolic solar receiver. Their numerical results show the effects of Grashof number and temperature ratio. The interaction of natural convection and surface radiation in flat-bottomed parabolic chambers is studied numerically by Diaz and Winston [9]. To obtain a solution of the fluid flow and heat transfer rate inside the non-rectangular enclosure, they applied a coordinate transformation that maps the parabolic domain to a rectangular domain by Dia and al[10]. In the early eighties, the attention of researchers was drawn to the study of natural convection in a differentially heated cavity inclined concerning a horizontal plane. The inclination has a very important effect on the structure of fluid flows and the rate of heat transfer. Among the ...

He conducted a two-dimensional numerical calculation based on the finite volume method and examined the influence of Rayleigh number and tilt angle on flow structure and convection heat transfer rate. The results obtained indicate a good agreement between the numerical results and the experimental measurements. On the other hand, correlations of the Nusselt number as a function of the Rayleigh number for different angles of inclination have been proposed. D.C. Lo et al. [11] used a new algorithm based on the differential quadrature method (DQ) proposed by Bellman. This method is applied by Shu and Xue [12] for the determination of the relative velocity of vortices and temperature variations of a natural convection flow of air confined in an inclined and differentially heated cubic cavity. They examined the effect of tilt on the heat transfer rate characterized by the Nusselt number. Khudheyer S. Mushatet [13] numerically studied heat transfer and fluid flow inside an inclined square cavity having two differentially heated corrugated vertical walls and two insulated flat horizontal walls. He studied the effect of tilt angle, amplitude, and ripple number for Rayleigh. The results obtained show that the rate of heat transfer increases with the increase in the number of ripples, the angle of inclination, and the Rayleigh number, on the other hand, the increase in the amplitude of the cavity decreases the number of local Nusselt and therefore the rate of heat transfer. A numerical study of two-dimensional natural laminar convection in a steady state in an enclosure formed by three cylinders is presented by Tahri et al. [14]. The bottom, which is represented by the two inner cylinders is heated by a heat flow of constant density, and the upper wall is formed by the outer cylinder.

Yahiaoui Abdelaziz [15] studied the phenomenon of natural convection in a laminar and permanent regime in a curved enclosure having two vertical curved active walls and two horizontal curved inactive walls, oriented at an angle he compared with the square enclosure. He studied the effect of the angle of inclination for Rayleigh numbers ranging from. The results obtained show that the curvature of the walls affects heat transfer. After studying convection in an enclosure where the lower wall is fully heated [16], the main objective of the present study will be to examine variations in the Nusselt number as a function of tilt angle. In addition to a practical interest in solar collectors, the study of natural convection in an enclosure bounded by two paraboloids of revolution is of academic interest because of the lack of studies on this geometry.

Abdelkrim Fatima [18] numerically studied laminar and steady-state thermal natural convection in a closed square cavity. The results are presented in the form of isotherms, vertical velocities, and streamlines, as well as the Nusselt number as a function of several Rayleigh number values (from 10^3 to 10^6). The obtained results show that an increase in the Rayleigh number enhances heat transfer by convection in the cavity. The influences of the volume fraction (ϕ) on convective flow, as well as the effect of the cavity's inclination (γ) on thermal performance, were examined by CHARAFI et al. [19]. The influence of inclination on thermal enhancement showed that the transfer becomes more efficient with an inclination of $\pi/6$. Bendaraa et al. [20] numerically studied the phenomenon of natural convection in a square cavity filled with a copper-water nanofluid. The studied domain is a square cavity with isothermal hot and cold walls at $x = 0$ and $x = L$, respectively, while the other walls are adiabatic. They examined the situation for Rayleigh numbers ranging from 10^4 to 10^6. They found that adding fins to the cold and adiabatic walls leads to an increase in the average Nusselt number, while it decreases when the fin is located on the hot wall. DOUBBI BOUNOUA Karim [21] analyzed pure natural convection and performed simulations for different Rayleigh numbers ($Ra = 10^3, 10^4, 5 \times 10^4, 10^5$). The results are presented in the form of streamlines, isotherms, velocity, and temperature profiles. Mohamed Chaour et al. [22] presented a two-dimensional numerical study of mixed laminar convection phenomena of nanofluids in a horizontal planar channel filled with water and different nanoparticles (Cu-water, Al_2O_3-water) for a nanoparticle volume fraction (φ) ranging from 0 to 0.2. The lower wall dissipates heat at a constant hot temperature, and the upper wall is considered adiabatic. The obtained results show that increasing the nanoparticle volume fraction (φ) promotes the heat transfer rate and has significant effects on the flow structure and the average Nusselt number, with Cu-water nanofluid being a better heat carrier compared to Al_2O_3-water nanofluid. Recently, ABBOU Benaouda [22] numerically examined the impact of the aspect ratio and non-uniform temperature on mixed convection in an enclosure. The chosen shape is an enclosure with a sinusoidal temperature on its lower wall, while the upper wall is considered adiabatic. The lateral walls of the cavity move downward with a uniform temperature TC. The inspection is carried out for several Richardson numbers and aspect ratios (Ar) varying from 0.25 to 5, while the Prandtl ($Pr = 0.71$) and Grashof ($Gr = 10^4$) numbers remain constant. The distributions of isotherm flux, streamlines, and Nusselt numbers inside the enclosure are highlighted and discussed.

2. Mathematical Formulation

2.1 Physical Model and Assumptions

Consider an enclosure bounded by two portions of cylindrical parabolas of horizontal axes open to the left and right and by a horizontal flat wall, filled with a Newtonian fluid in this case air (see Figure 1).

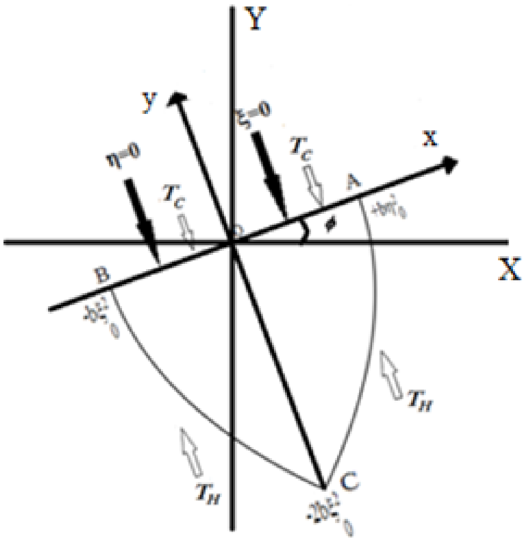

Figure 1. Configuration of the geometry studied.

The cavity being haeted differently a convection phenomenon takes birth inside the enclosed space. To formulate and solve this problem it is assumed that:

All the phenomena are independent of the time;

The fluid is Newtonian and the flow is laminar;

The phenomena are two-dimensional;

All fluid properties are taken to be constant, with the exception of the density in the momentum equation. In this equation variations of density obey the Boussinesq linear law;

In the heat equation, the viscous dissipation and the compression effects are neglected.

Under these conditions, the transfer equations in a cartesian coordinates system are:

Stream function equation:

$$\omega = -\left\{\frac{\partial^2\psi}{\partial x^2}+\frac{\partial^2\psi}{\partial y^2}\right\} \tag{1}$$

Momentum equation:

$$\left\{u_x\frac{\partial\omega}{\partial x}+u_y\frac{\partial\omega}{\partial y}\right\} = \beta g\left\{\cos\phi\ \frac{\partial\left(T-T_0\right)}{\partial x}-\sin\phi\frac{\partial\left(T-T_0\right)}{\partial y}\right\}+\nu\left\{\frac{\partial^2\omega}{\partial x^2}+\frac{\partial^2\omega}{\partial y^2}\right\} \tag{2}$$

Heat equation:

$$\left\{u_x\frac{\partial T}{\partial x}+u_y\frac{\partial T}{\partial y}\right\} = \alpha\left\{\frac{\partial^2 T}{\partial x^2}+\frac{\partial^2 T}{\partial y^2}\right\} \tag{3}$$

Where: $u_x = \frac{\partial\psi}{\partial y}$ and $u_y = -\frac{\partial\psi}{\partial x}$

To resolve our problem, it is more convenient to use a curvilinear system of coordinates more adapted to the shape of our cavity.

In this system of coordinates:

- The parabolic surfaces are respectively located by the coordinates lines $\eta=\eta_0$ and $\xi=\xi_0$;
- The horizontal plane wall is located by the two lines of coordinates $\eta = 0$ $\xi = 0$.

The passage to a curvilinear coordinate is carried out using the following relations:

$$\vec{V} = u_x \vec{e}_x + u_y \vec{e}_y = u_\xi \vec{e}_\xi + u_\eta \vec{e}_\eta \tag{4}$$

with:

$$\begin{cases} \vec{e}_\xi = 2b\left(-\xi \vec{e}_x + \eta \vec{e}_y\right) \\ \vec{e}_\eta = 2b\left(\eta \vec{e}_x + \xi\eta \vec{e}_y\right) \end{cases} \tag{5}$$

u_x and u_y are connected to u_η and u_ξ by the relations:

$$\begin{cases} u_x = 2b\left(-\xi u_\xi + \eta u_\eta\right) \\ u_y = 2b\left(-\eta u_\xi + \xi u_\eta\right) \end{cases} \tag{6}$$

b is the shape factor of our cavity. By taking into account the law of transformation of coordinates, it comes that:

$$\begin{cases} \dfrac{\partial}{\partial x} = \dfrac{2b}{h^2}\left(\eta \dfrac{\partial}{\partial \eta} - \xi \dfrac{\partial}{\partial \xi}\right) \\ \dfrac{\partial}{\partial y} = \dfrac{2b}{h^2}\left(\xi \dfrac{\partial}{\partial \eta} - \eta \dfrac{\partial}{\partial \xi}\right) \end{cases} \tag{7}$$

with $h'^2 = 4b^2\left(\eta^2 + \xi^2\right)$

In the curvilinear system of coordinates the equation of transfer in a non-dimensional form is:

$$\omega = -\frac{1}{(h)^2} . \left\{\frac{\partial^2 \psi}{\partial \xi^2} + \frac{\partial^2 \psi}{\partial \eta^2}\right\} \tag{8}$$

Momentum equation:

$$h\left\{\frac{\partial}{\partial \eta}\left(h.\, \mathrm{V}_\eta .\, \omega\right) + \frac{\partial}{\partial \xi}\left(h.\, \mathrm{V}_\xi .\, \omega\right)\right\} = \frac{\beta.\, \mathrm{g}}{h.\, h_0}\left\{\begin{matrix}\left[\xi.\, \cos\phi + \eta.\, \sin\phi\right].\dfrac{\partial T}{\partial \eta} + \\ \left[\eta.\, \cos\phi - \xi.\, \sin\phi\right].\dfrac{\partial T}{\partial \xi}\end{matrix}\right\} + \frac{\nu}{h^2}.\left\{\frac{\partial^2 \omega}{\partial \eta^2} + \frac{\partial^2 \omega}{\partial \xi^2}\right\} \tag{9}$$

Heat equation:

$$h\left\{u_\xi \frac{\partial \theta}{\partial \xi} + v_\eta \frac{\partial \theta}{\partial \eta}\right\} = \left\{\frac{\partial^2 \theta}{\partial \xi^2} + \frac{\partial^2 \theta}{\partial \eta^2}\right\} \tag{10}$$

with:

$$\begin{cases} u_\xi = -\dfrac{1}{h}.\dfrac{\partial \psi}{\partial \eta} \\ V_\eta = \dfrac{1}{h}.\dfrac{\partial \psi}{\partial \xi} \end{cases}$$

To write the equations in a non-dimensional form, we have defined the following value of reference:

- $L = 2b$ the length of reference;
- $u_{ref} = \dfrac{\alpha}{L}$ the velocity of reference.

We also define two parietal coefficients: the Nusselt number (Nu) and the friction coefficient (Cf).
These two coefficients are calculated on the two parabolic walls:

$$Nu = -\frac{1}{1-\bar{\theta}_f}\frac{\partial \theta}{\partial(\eta,\xi)}_{\eta=\eta_m,\xi=\xi_m} \tag{11}$$

$$Cf = \frac{2.Pr}{h}.\frac{\partial(u_\eta,u_\xi)}{\partial(\eta,\xi)}_{\eta=\eta_m,\xi=\xi_m} \tag{12}$$

$\vec{\theta}$ is the average temperature inside the enclosure.
The boundary conditions associated with our problem are:

- at $\eta = \eta_0$:

$$\varpi = \frac{1}{h^2}\frac{\partial^2\psi}{\partial\eta^2}\bigg|_{\eta=\eta_0} \tag{13}$$

$$\theta=1 \tag{14}$$

$$u_\xi = v_\eta = \psi = \frac{\partial\psi}{\partial\eta}\bigg|_{\eta=\eta_0} = \frac{\partial\psi}{\partial\xi}\bigg|_{\eta=\eta_0} = 0 \tag{15}$$

- at $\eta = 0$:

$$\varpi = -\frac{1}{h^2}\frac{\partial^2\psi}{\partial\eta^2}\bigg|_{\eta=0} \tag{16}$$

$$\theta = 0 \tag{17}$$

$$u_\xi = v_\eta = \psi = \frac{\partial\psi}{\partial\eta}\bigg|_{\eta=0} = \frac{\partial\psi}{\partial\xi}\bigg|_{\eta=0} = 0 \tag{18}$$

- at $\xi = \xi_0$:

$$\varpi = -\frac{1}{h^2}\frac{\partial^2\psi}{\partial\xi^2}\bigg|_{\xi=\xi_0} \tag{19}$$

$$\theta = 1 \tag{20}$$

$$u_\xi = v_\eta = \psi = \frac{\partial\psi}{\partial\eta}\bigg|_{\xi=\xi_0} = \frac{\partial\psi}{\partial\xi}\bigg|_{\xi=\xi_0} = 0 \tag{21}$$

- at $\xi = 0$:

$$\varpi = -\frac{1}{h^2}\frac{\partial^2\psi}{\partial\xi^2}\bigg|_{\xi=0} \tag{22}$$

$$\theta = 0 \tag{23}$$

$$u_\xi = v_\eta = \psi = \frac{\partial\psi}{\partial\eta}\bigg|_{\xi=0} = \frac{\partial\psi}{\partial\xi}\bigg|_{\xi=0} = 0 \tag{24}$$

3. Numerical Formulation

The equations that describe the behavior of the fluid are solved by Polynomial Differential Quadrature method (PDQ) [9-11].

The governing equations discretized by employing a PDQ method become as follows:

Equation of Vorticity:

$$-\varpi_{i,j}=-\frac{1}{h_{i,j}^{2}}\left[\sum_{k}^{N}b_{i,k}\psi_{k,j}+\sum_{k}^{M}\bar{b}_{j,k}\psi_{i,k}\right] \tag{25}$$

Equation of momentum:

$$h_{i,j}\left[u_{i,j}\sum_{k}^{N}a_{i,k}\varpi_{k,j}+v_{i,j}\sum_{k}^{M}\bar{a}_{j,k}\varpi_{i,k}\right]=\Pr\left[\sum_{k}^{N}b_{i,k}\varpi_{k,j}+\sum_{k}^{M}\bar{b}_{j,k}\varpi_{i,k}\right]+Ra\Pr\left[\begin{array}{l}\cos\phi\left(\eta_{j}\sum_{k}^{M}\bar{a}_{j,k\,\theta_{i,k}}-\xi_{i}\sum_{k}^{N}a_{i,k}\theta_{k,j}\right)-\\ \sin\phi\left(\xi_{i}\sum_{k}^{M}\bar{a}_{j,k}\theta_{i,k}+\eta_{j}\sum_{k}^{N}a_{i,j}\theta_{k,j}\right)\end{array}\right] \tag{26}$$

Heat equation:

$$h_{i,j}\left[u_{i,j}\sum_{k}^{N}a_{i,k}\theta_{k,j}+v_{i,j}\sum_{k}^{M}\bar{a}_{j,k}\theta_{i,k}\right]=\left[\sum_{k}^{N}b_{i,k}\theta_{k,j}+\sum_{k}^{M}\bar{b}_{j,k}\theta_{i,k}\right] \tag{27}$$

Where the indices i,j indicate a grid point, and N,M represent the total number of grid points in ξ η and directions respectively. $a_{i,k}$, $b_{i,k}$ are the weighting coefficients of the first and the second derivatives in the ξ direction; $\bar{a}_{j,k}$, $\bar{b}_{j,k}$ are also the weighting coefficients of the first and second order derivatives but in the η direction. The gird points are generated by the Tchebychev-Gauss-Lobatto Quadrature:

$$\begin{cases}\xi_{i}=\frac{1}{2}\left[1-\cos\left(\frac{i-1}{N-1}\right)\pi\right] & \text{i = 1...N}\\ \eta_{j}=\frac{1}{2}\left[1+\cos\left(\frac{j-1}{M-1}\right)\pi\right] & \text{j = 1...M}\end{cases} \tag{28}$$

For the computation of the weighting coefficients, we can see [13]. For each value of the Rayleigh number (R_a) and the slope angle (ϕ), different grid sizes have been tested in order to know the influence of the mesh size on the results. The systems of algebraic equations resulting from the discretization are solved by a Successive over-relaxation method (SOR). The iteration process is terminated if the following criterion is satisfied:

$$\frac{\left|\sum_{i,j}\left(F_{i,j}^{k+1}\right)-\sum_{i,j}F_{i,j}^{k}\right|}{\left|\sum_{i,j}F_{i,j}^{k+1}\right|}\leq\varepsilon \tag{29}$$

With k the incrementing index of the iteration process, ε his precision and F function can be represent ϖ, θ or ψ ed.

4. Results and Discussions

The calculation code we have developed is transcribed in Fortran and the various scripts used to process the data are written in Python. This calculation code is executed on a microcomputer with a speed of 2.16GHZ and a RAM of 3.89 GB. The execution time is very short We validated our calculation code by comparing our calculation steps with those from the literature. As an example, we adopted the approach used by Shu (17) to solve these types of equations. Heat transfers are examined for Rayleigh numbers between 10^4 and 10^5 and various angles of inclination of the enclosure ($\phi=0;\pi/4;\pi/2;3\pi/4;5\pi/6;\pi$). Throughout the simulation the Prandtl number is fixed at 0.7, the form factor b is equal to 1/2 and we take for $\eta_0 = \xi_0 = 1$.

We will vary only two quantities:

The Nusselt number,

The angle of the inclination ϕ.

Tilt angle is an important physical parameter that can impact the Nusselt number. The angle at which a surface is tilted can affect the heat transfer rate from the surface to the surrounding fluid. As the tilt angle increases, the flow of the fluid is altered, which can lead to changes in the Nusselt number. Therefore, it is important to consider the effects of tilt angle when studying heat transfer phenomena.

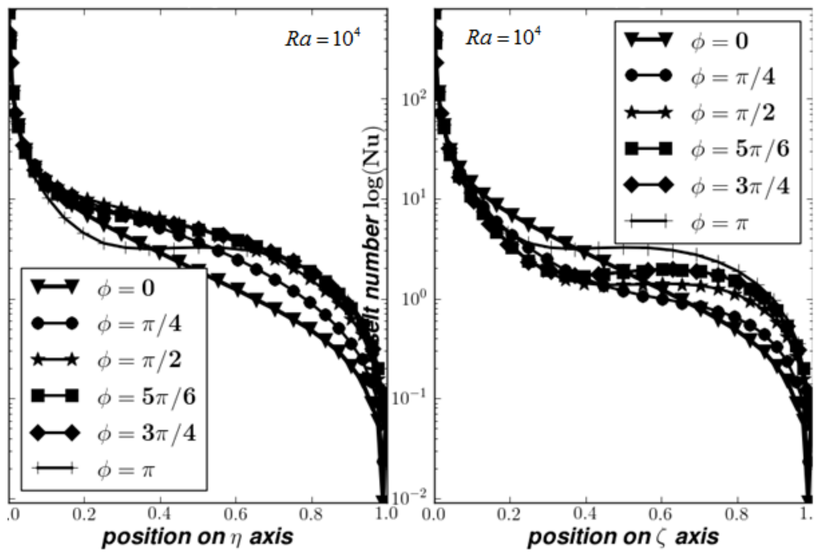

Figure 2. Variation in the number of local Nusselts on the walls for $R_a = 10^4$.

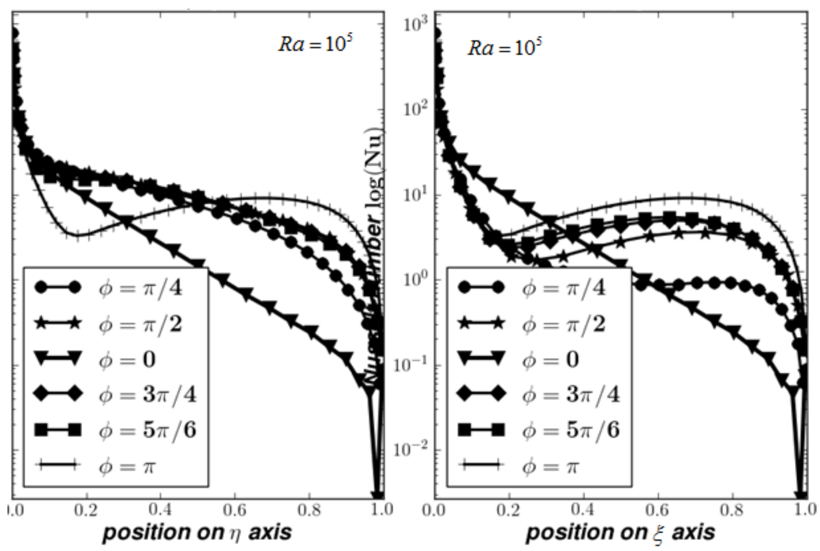

Figure 3. Variation in the number of local Nusselt on the walls $R_a = 10^5$.

Figures 2 and 3 represent the influences of inclination and Rayleigh number on variations in local Nusselt numbers (characterizes the ability of the fluid to extract heat on the walls). The numerical results were obtained in the range of values of the Rayleigh number $Ra = 10^4$ $Ra = 10^5$. We notice that the Nusselt numbers on both walls decrease rapidly as one moves away from the points or approaches the angular point represented by C. Indeed, at this point the coordinate lines $\eta = cte$ et $\xi = cte$ are perpendicular and are at the same temperature so the heat exchange is zero at this point. Then it begins to decrease until it reaches its minimum 10^{-2} at the top of the wall.

This means that the rates of heat transfer given via the local Nusselt number are important at this location $\eta = 0$ et $\xi = 0$. It is less important at the other place of the wall where $\eta = 1$ et $\xi = 1$. For $R_a = 10^5$ et $\phi = 0$, we note that whatever the wall is considered, the rate of heat transfer between the walls and the fluid is important.

For $\phi = \pi$ corresponds to the lowest transfers and the least intense transfers correspond to tilt angles $\phi = \frac{\pi}{4}, \frac{\pi}{2}, \frac{3\pi}{4}, \frac{5\pi}{6}$. Because of symmetry, the same phenomenon occurs on both sides of the wall.

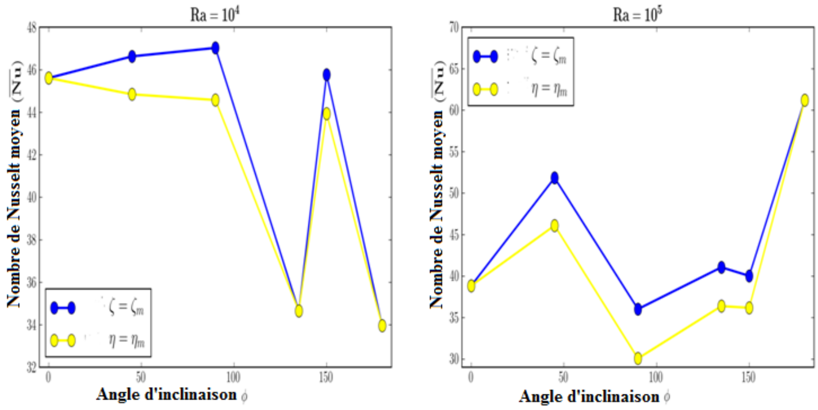

Figure 4. Variations $\overline{Nu}$ on the two parabolic walls.

In Figure 4, $Ra = 10^4$ we can note that whatever the wall is considered, heat transfers between the parabolic walls and the fluid are important $\phi \le \frac{\pi}{2}$. The most intense transfers correspond to $\phi = \frac{\pi}{2}$ and the weakest is the inclination $\phi = \pi$. For $Ra = 10^5$, contrary to the previous case $\phi = \pi$ convective exchanges are more intense and weaker with inclination $\phi = \frac{\pi}{2}$.

5. Conclusion

In this work, we investigated the effect of the Nusselt number as a function of the angle of inclination ϕ on heat transfer within an enclosure bounded by two cylindrical parabolas of the horizontal generator and a flat surface. From the analysis of the different results obtained we can conclude that:

The transition from a pseudo-conductive $\left(Ra \le 10^4\right)$ state to a convective $\left(Ra \ge 10^5\right)$ state is little influenced by the angle of inclination ϕ.

$Ra = 10^4$ The most intense transfers correspond to $\phi = \frac{\pi}{2}$ and the weakest for. The most intense transfers correspond to and the weakest for $\phi = \pi$.

$Ra = 10^5$ The most intense transfers correspond to $\phi = \frac{\pi}{2}$ and the weakest for. The most intense transfers correspond to and the weakest for $\phi = \pi$.

The tilt angle is an important physical parameter that impacts the Nusselt number. The angle of inclination of the surface affected the heat transfer rate from the surface to the surrounding fluid. As the tilt angle increases, the fluid flow is changed, resulting in the variation of the Nusselt number. Therefore, the effects of the angle of inclination were taken into account when studying heat transfer phenomena.

We find that natural convection becomes increasingly important as Rayleigh numbers increase. An interesting continuation of this work would be to take more complex geometrics and other types of fluids by generalizing the developed algorithm. But also, applies other boundary conditions such as a heat flux density varying with time.

Nomenclature

List of Symbols

Latin Letters

b : Form factor
Cf : Coefficient of friction
$\overline{C}f$: Average coefficient of friction
g : Acceleration of gravity $\left[m.s^{-2}\right]$
h : Metric coefficient
L : Reference length $\left[m\right]$
Nu : Nusselt number
$\overline{Nu}$: Average Nusselt number
Pr : Prandtl number $\Pr : \frac{\nu}{\alpha}$
Ra : Rayleigh number $Ra : \frac{\beta g\left(T_h - T_c\right)L^3}{\alpha \eta_{vis}}$
S : Area of the enclosure $\left[m^2\right]$
t : Dimensionless time
U, V : Components of dimensionless velocities
x, y : Cartesian coordinates[m]
$\vec{n}$: Vector normal to the wall
Cp : Mass heat capacity $\left[J.Kg^{-1}.K^{-1}\right]$
T: temperature [K]
T_0 : reference temperature [K]
P : pressure $\left[P_a\right]$
V_N : Linear vector space
$r_k(x)$: Polynomials
$c_0, c_1, ...c_{N-1}$: Constants
$x_1, x_2 ....x_N$: Coordinates of mesh points
$a_{ii}, b_{jj}, w_{jk}, w_{ik}, w_{kj}$: Weighting coefficients
$w_{i,k}^{(2)}, w_{j,k}^{-(2)}, w_{i,k}^{(1)}, w_{j,k}^{-(1)}$: The coefficients corresponding to the discretization of derivatives

Greek Letters

α : Thermal diffusivity of the fluid $\left[m^2.s^{-1}\right]$
β : Coefficient of thermal expansion $\left[K^{-1}\right]$
ϕ : Angle of inclination $\left[rad\right]$
η, ξ : Parabolic coordinates
η_{vis} : Kinematic viscosity $\left[m^2 s^{-1}\right]$
λ : Thermal conductivity $\left[Wm^{-1}K^{-1}\right]$
ν : kinematic viscosity $\left[m^2 s^{-1}\right]$

ϖ : Dimensionless vorticity

θ : Dimensionless temperature $\theta = (T - T_c)/(T_h - T_c)$

Ψ : Dimensionless current function

ε : Calculation accuracy

Indices

i, j : Discretization Indices:

k : Incrementation Index of the Iteration Process

References

[1] G.DE Vahl Davis. Laminar natural convection in an enclosed rectangular cavity. Int. J. Heat Mass Transfer, 1960, vol.ll, pp. l675-1693.

[2] G. De Vahl Davis. Natural convection of air in a square cavity: A benchmark numerical solution. International Journal for Numerical Methods in Fluids, 3, pp. 249-264, 1983.

[3] M. Kaviany. Effect of a Protuberance on Thermal Convection in a Square Cavity. Journal of Heat Transfer, Vol. 106, n. 1, pp. 830-834, 1984.

[4] W. M. Lewandowski, M. J. Khubeiz, Experimental Study of Laminar Natural Convection in Cells With Various Convex and Concave Bottoms. Journal of Heat Transfer, Vol. 114, n. 1, pp. 94-98, 1992.

[5] S. Najoua, C. Mbow, J. H. Lee, W. H. Park, M. Daguenet. Étude Numérique du Modèle de Boussinesq de Convection Naturelle Laminaire Transitoire dans un Ellipsoïde de Révolution de grand Axe Vertical Rempli d'Air (Numerical Study of the Boussinesq Model of Transient Laminar Natural Convection in a Vertically Elongated Ellipsoid Filled with Air). Revue Générale de Thermique, Vol. 36, n. 3, pp. 224-233, 1997.

[6] S. Das, Y. Morsi, Natural Convection Inside Dome Shaped Enclosures. International Journal of Numerical Methods for Heat & Fluid Flow, Vol. 12, n. 2, pp. 126-141, 2002.

[7] Y. Morsi, S. Das. Numerical Investigation of Natural Convection inside Complex Enclosures. International Journal of Numerical Methods for Heat & Fluid Flow, Vol. 24, n. 2, pp. 30-41, 2003.

[8] N. S. Kumar, K. S. Reddy. Investigation of Convection and Radiation Heat Losses From Modified Cavity Receiver of Solar Parabolic Dish Using Asymptotic Computational Fluid Dynamics. Heat Transfer Engineering, Vol. 31, n. 7, pp. 597-607, 2010.

[9] G. Diaz, R. Winston. Effect of Surface Radiation on Natural Convection in Parabolic Enclosures. Numerical Heat Transfer, Part A, Vol. 53, n. 9, pp. 891-906, 2008.

[10] A. W. Mustafa. Natural convection in Parabolic Enclosure Heated from Below. Modern Applied Science, Vol. 5, n. 3, pp. 213-220, 2011.

[11] D.C. Lo, D.L. Young, K. Murugesan, C.C. Tsai, M.H. Gou. Velocity–vorticity formulation for 3D natural convection in an inclined cavity by DQ method, 2007.

[12] Shu, C. and Xue, H. Explicit computation of weighting coefficients in the harmonic differential quadrature. J Sound Vib, 204(3), 549-555, (1997).

[13] Khudheyer S. Mushatet. Simulation of Natural Convection in an Inclined Square Cavity with Two Wavy Walls. Journal of Applied Sciences Research, 6(12): 2111-2122, (2010).

[14] B.Tahri, K. Bouhadef, A. Slimani Et M. Rebhi. Effet de l'inclinaison sur la convection naturelle dans un espace forme par trois cylindres, 10ème Séminaire International Sur La Physique Energétique (Effect of Inclination on Natural Convection in a Space Formed by Three Cylinders, 10th International Seminar on Energy Physics). Journal of Scientific Research, N° 0 vol. 1, (2010).

[15] Yahiaoui Abdelaziz. Etude de la convection naturelle dans les enceintes courbées ayant deux parois actives courbées verticales et deux parois inactives courbées horizontales; Mémoire, Université Mentouri Constantine, Faculté des Sciences Exactes département de physique-Algérie 2012 (Study of natural convection in curved enclosures with two active curved vertical walls and two inactive curved horizontal walls; Thesis, Mentouri University Constantine, Faculty of Exact Sciences, Department of Physics – Algeria 2012).

[16] S. Dia, C. Mbow and J. Sarr. Effects of the Heater Location on the Unsteady Two-Dimensional Natural Convection in Enclosure Bounded by Two Paraboloids of Revolution. American Journal of Fluid Dynamics, Vol.3, N.3, p 49-57, 2013.

[17] C. Shu. Application of Differential Quadrature to Simulate Natural Convection in a Concentric Annulus. Int. J. Numer. Meth. Fluids, 30: 977-993 (1999).

[18] Abdelkrim Fatima. Mémoire sur l'Etude de la convection naturelle thermique dans une enceinte fermée (Memoir on the Study of Natural Thermal Convection in a Closed Enclosure), 2018.

[19] M.M. Charafi, A. Bendaraa, A. Hasnoui. Numerical Modelling of Natural Convection in Square Cavity Filled with Effect of Nanofluid Volume Fraction and Inclination. J. MATEC Web of Conferences (2018). https://doi.org/10.1051/matecconf/201824101006.

[20] A. Bendaraa, Mly. M. Charafi, A. Hasnaoui. Numerical Study Of Natural Convection In A Differentially Heated Square Cavity Filled With Nanofluid In the Presence of Fins Attached To Walls In Different Locations. J. Physics of Fluids, 2019. https://doi.org/10.1063/1.5091709.

[21] Doubbi Bounoua Karim. Analyse de la Convection Naturelle dans une enceinte rectangulaire chauffée discrètement par le bas. 2022 (Analysis of Natural Convection in a Rectangular Cavity Heated Discretely from the Bottom. 2022).

[22] Mohamed Chaour, Sofiane Boulkroune, Billel Hamadi, Toufik Achour, Djamel Boucherma. Étude numérique du transfert de chaleur des nanofluides dans un canal plan application au panneau solaire thermique (Numerical study of heat transfer of nanofluids in a flat channel application to solar thermal panels). Journal of Physical & Chemical Research, 2023. https://ojs.univ-bba.dz.

[23] Abbou Benaouda. Mémoire sur l'Analyse numérique de l'influence des caractéristiques géométrique et thermique sur le transfert par convection mixte dans les enceintes, 2024 (Thesis on the Numerical Analysis of the Influence of Geometric and Thermal Characteristics on Mixed Convection Transfer in Enclosures, 2024).